JACS
JOURNAL OF THE AMERICAN CHEMICAL SOCIETY
Article
pubs.acs.org/JACS

Formation Mechanisms, Structure, Solution Behavior, and Reactivity of Aminodiborane

Huizhen Li,[†,⊥] Nana Ma,[†,⊥] Wenjuan Meng,[†] Judith Gallucci,[‡] Yongqing Qiu,[∥] Shujun Li,[†] Qianyi Zhao,[†] Jie Zhang,[*,†] Ji-Cheng Zhao,[*,§] and Xuenian Chen[*,†]

[†]Key Laboratory of Green Chemical Media and Reactions, Ministry of Education, Collaborative Innovation Center of Henan Province for Green Manufacturing of Fine Chemicals, School of Chemistry and Chemical Engineering, Henan Normal University, Xinxiang, Henan 453007, China

[‡]Department of Chemistry and Biochemistry, and [§]Department of Materials Science and Engineering, The Ohio State University, Columbus, Ohio 43210, United States

[∥]Faculty of Chemistry, Northeast Normal University, Changchun, Jilin 130024, China

Supporting Information

ABSTRACT: A facile synthesis of cyclic aminodiborane ($NH_2B_2H_5$, ADB) from ammonia borane ($NH_3{\cdot}BH_3$, AB) and THF·BH_3 has made it possible to determine its important characteristics. Ammonia diborane ($NH_3BH_2(\mu\text{-}H)BH_3$, AaDB) and aminoborane (NH_2BH_2, AoB) were identified as key intermediates in the formation of ADB. Elimination of molecular hydrogen occurred from an ion pair, $[H_2B(NH_3)(THF)]^+[BH_4]^-$. Protic-hydridic hydrogen scrambling was proved on the basis of analysis of the molecular hydrogen products, ADB and other reagents through ^2H NMR and MS, and it was proposed that the scrambling occurred as the ion pair reversibly formed a BH_5-like intermediate, $[(THF)BH_2NH_2](\eta^2\text{-}H_2)BH_3$. Loss of molecular hydrogen from the ion pair led to the formation of AoB, most of which was trapped by BH_3 to form ADB with a small amount oligomerizing to $(NH_2BH_2)_n$. Theoretical calculations showed the thermodynamic feasibility of the proposed intermediates and the activation processes. The structure of the ADB·THF complex was found from X-ray single crystal analysis to be a three-dimensional array of zigzag chains of ADB and THF, maintained by hydrogen and dihydrogen bonding. Room temperature exchange of terminal and bridge hydrogens in ADB was observed in THF solution, while such exchange was not observed in diethyl ether or toluene. Both experimental and theoretical results confirm that the B−H−B bridge in ADB is stronger than that in diborane (B_2H_6, DB). The B−H−B bridge is opened when ADB and NaH react to form sodium aminodiboronate, $Na[NH_2(BH_3)_2]$. The structure of the sodium salt as its 18-crown-6 ether adduct was determined by X-ray single crystal analysis.

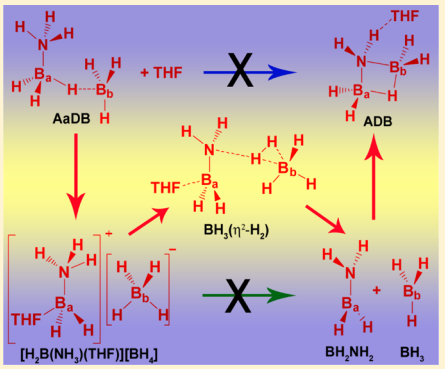

1. INTRODUCTION

Aminodiborane ($NH_2B_2H_5$, ADB) is a strained cyclic amine borane derived from diborane (B_2H_6, DB) in which one of the two bridge hydrogens has been replaced by an amino group (NH_2). With reactivity similar to DB, broad application of ADB can be expected in both organic and inorganic syntheses.[1] Although ADB has been little studied, a recent report of the facile synthesis of ADB by a catalyst-free reaction between ammonia borane ($NH_3{\cdot}BH_3$, AB) and tetrahydrofuran borane (THF·BH_3) may now enable its greater investigation.[1a] Of critical importance to the aforementioned synthetic method of Shore is its potential generality.[1e] This new method has already been used to synthesize other N-substituted aminodiboranes from the appropriate N-substituted amineboranes[1b,c] and $PhNHB_2H_5$ from reactions of $PhNH_2{\cdot}BH_3$ with THF·BH_3 or $(CH_3)_2S{\cdot}BH_3$.[1d] However, the precise mechanism underlying this method is not well understood. On the other hand, the N-substituted aminodiboranes can be synthesized by the reactions of DB with N-substituted aminoboranes or their corresponding lithium amides,[2,3] but these methods are not suitable for synthesizing ADB. When unsubstituted aminoborane (NH_2BH_2, AoB)[4] forms, it rapidly polymerizes, which may account for the difficulty of preparation of ADB by this route. Monomeric primary aminoboranes and related secondary aminoboranes with small substituents are elusive as they readily dimerize/oligomerize.[1e] Collectively, this data inspired us to initiate a comprehensive investigation of the mechanism of the reaction between AB and THF·BH_3.

As shown in Scheme 1, initial nucleophilic addition of a B−H of AB displaces THF from THF·BH_3 to form ammonia diborane ($NH_3BH_2(\mu\text{-}H)BH_3$, AaDB). Subsequently, intermediate AaDB loses molecular hydrogen and ADB is formed. Direct observation of AaDB has been accomplished by ^{11}B NMR during the reaction of AB and THF·BH_3 and is consistent with the formation of a stabilizing dihydrogen

Received: August 7, 2015
Published: September 3, 2015

DOI: 10.1021/jacs.5b08033
J. Am. Chem. Soc. 2015, 137, 12406−12414

Scheme 1. Formation of ADB by Reaction of AB and THF·BH_3

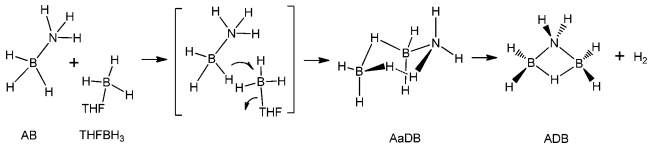

bond (DHB) which promotes the loss of molecular hydrogen.[5] In the present study, we have carried out both experimental and theoretical studies in order to confirm important aspects of the mechanism in which AaDB loses molecular hydrogen to form ADB.

Single crystal X-ray diffraction analysis shows that the crown ether adduct of ADB, 18-crown-6 aminodiborane, 2ADB·$C_{12}H_{24}O_6$, is triclinic and belongs to the $P\bar{1}$ space group.[1a] Here we report the X-ray single crystal structures of ADB·THF and the sodium salt of aminodiborane, $Na[NH_2(BH_3)_2]$. NMR experiments have been conducted to characterize the hydrogen exchange behavior of ADB, which is similar to that of *N*-methyl aminodiborane but much different from that of DB.

2. RESULTS AND DISCUSSION

2.1. Preparation of ADB and Its Analogues. Why Has the Availability of ADB Been so Limited? Until recently there had been no suitable alternative to the original synthesis of ADB reported in 1938,[6] a synthesis requiring challenging conditions and affording only low yields. Recently, Shore et al. reported a convenient preparation of ADB in moderately high yields by the reaction of AB with THF·BH_3 at room temperature.[1a] In contrast, the *N*-methyl analogues are conveniently synthesized by the reaction of the appropriate *N*-methyl aminoboranes, obtained by dehydrogenation of the corresponding *N*-methyl amineboranes, with DB: *N,N*-dimethyl aminodiborane from direct addition of *N,N*-dimethyl aminoborane ($(CH_3)_2NBH_2$) to DB;[2a] *N*-methyl aminodiborane from direct addition of *N*-methyl aminoborane (CH_3NHBH_2) to DB.[2a] Although only partial polymerization of *N*-methyl aminoborane (CH_3NHBH_2) was observed, dehydrogenation of AB to form AoB results in complete and rapid polymerization of AoB. The N-substituted aminodiboranes can also be obtained in good yield by the stepwise addition of DB to diethyl ether solutions of $LiN(CH_3)_2$ at room temperature or $LiNH(CH_3)$ at 0 °C or below.[3a] Under the same conditions, excess DB was bubbled into an ether slurry of $LiNH_2$ and an AoB polymer of empirical composition $(NH_2BH_2)_n$ was obtained, rather than ADB.[3b,c] Cyclic aminoboranes ($(NH_2BH_2)_n$, n = 2, 3, 4, 5) are obtained in the reaction between $NaNH_2$ and the diammoniate of diborane ($[H_2B(NH_3)_2][BH_4]$, DADB) in liquid ammonia.[3d]

These experimental results indicate that aminoboranes ($RR'NBH_2$, R, R′ = H, alkyl) were first produced and their steric hindrance determined the final products. When both R and R′ are alkyl groups, sufficient steric hindrance prevents polymerization so that the $RR'NBH_2$ monomer persists to further react with a BH_3 group, producing an N-substituted aminodiborane. In contrast, when both R and R′ are H, the lessened steric hindrance renders AoB favorable toward self-polymerization.[3d,4,6b] The intermediate situation, where R = alkyl and R′ = H, $RR'N{=}BH_2$ represents an intermediary between the parent compound and its *N,N*-dialkyl derivatives, partially formed *N*-alkyl aminodiborane and partially formed *N*-alkyl aminoborane polymer.[3a,4a] Therefore, further insight into the markedly different reactivity of AoB from its *N*-methyl analogues is of significance for syntheses of B−N polymers and other amine borane complexes.

2.2. Formation Mechanism of ADB. DHB and proton−hydride exchange play an important role in amine borane chemistry, especially in dictating the reaction pathways (and thus different products distributions).[5,7,8] As set out in Scheme 1, formation of ADB is assisted by a stabilizing DHB formation in AaDB and by elimination of a dihydrogen molecule formed by a protonic amine hydrogen and a hydridic borane hydrogen.[1a] In this Article, experiments have been developed to investigate the role of DHB and proton-hydride scrambling in the formation of ADB from AB and THF·BH_3. Theoretical calculations have also been conducted to provide comprehensive insight into the formation mechanism of ADB.

2.2.1. Experiments to Confirm the Presence of the Intermediate, Aminoborane (NH_2BH_2, AoB). A small amount of white precipitate produced in the reaction of AB and THF·BH_3[1a] has now been identified as $(NH_2BH_2)_n$ (Figure S1).[9] This result confirms that AoB forms in the reaction, most of which is trapped by THF·BH_3 to form ADB, with a small amount oligomerizing to $(NH_2BH_2)_n$. An attempt to trap AoB by reaction with cyclohexene was unsuccessful. The characteristic signal of $NH_2B(Cy)_2$ at δ = 46.9 ppm in ^{11}B NMR was not observed[10] when cyclohexene was added along with AB and THF·BH_3. We suggest that the rate of AoB trapping by borane is more rapid than its hydroboration of the C=C double bond of cyclohexene. Thus, the steady-state concentration of AoB may be too low for the cyclohexene trapping experiment to work.

2.2.2. Reactions of N-Methyl Amineboranes with THF·BH_3. Many N-substituted aminodiboranes have been synthesized using similar preparation methods as ADB[1b−d] as well as by other routes.[2,3] In our study, *N*-methyl aminodiboranes were produced by reactions of *N*-methyl amineboranes with THF·BH_3 at room temperature and the reactions were monitored by NMR spectroscopy. Compared with the parent compound ADB, both the formation rates and conversions of *N*-methyl aminodiboranes decreased with the increasing methyl substitution (Figures 1 and S2−S5). Both steric hindrance to B−H addition by the *N*-methyl groups and reduction in the number of available N−H hydrogens to form stabilizing DHB interactions may be important factors. Steric hindrance is maximized in the case of *N,N,N*-trimethyl amineborane which has no N−H proton available for DHB formation. There is no

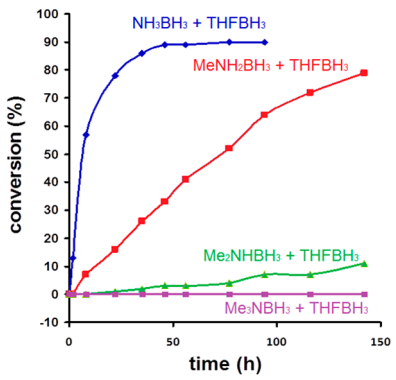

Figure 1. Different reaction rates and conversions between THF·BH_3 and NH_3·BH_3, $MeNH_2$·BH_3, Me_2NH·BH_3, and Me_3N·BH_3.

DOI: 10.1021/jacs.5b08033
J. Am. Chem. Soc. 2015, 137, 12406−12414

NMR evidence for the reaction between *N,N,N*-trimethyl amineborane and THF·BH_3 (Figure S5).

2.2.3. Hydrogen Scrambling/Exchange during the Formation of ADB. According to a well-accepted mechanism, two oppositely polarized hydrogens can interact with each other to form a molecular hydrogen coordination complex, via an ion pair intermediate in which a proton and hydride exchange reaction takes place and/or molecular H_2 may be released.[7f] In order to examine DHB and hydrogen scrambling and probe the mechanism for the formation of molecular hydrogen, two deuterium substituted reagents, ND_3·BH_3 and THF·BD_3 were used to synthesize ADB. Predictions based on the involvement of a DHB transition state are included in AaDB (Scheme 1) along with a qualitative report of the hydrogen isotopes detected by mass spectrometry. Elimination with no proton−deuteron scrambling produces only HD in both experiments. As can be seen from the qualitative indication of results, scrambling is the predominant process in both experiments (Figure S6).

When NH_3·BH_3 reacted with THF·BD_3, all three possible gas products H_2, HD, and D_2 were detected (Figure S6a). In addition to confirming the presence of THF·BD_3, NH_3·BD_3 and $NH_2B_2D_5$, signals consistent with deuterium at both hydride and proton positions in AB and ADB (Figure S6b), were observed.[1a,11] Scrambling had affected all hydrogen (hydride and proton) positions. When ND_3·BH_3 was reacted with THF·BH_3, H_2 and HD were formed (Figure S7a) according to ^{2}H NMR which not only affirmed the presence of ND_3·BH_3 and $ND_2B_2H_5$ but also included broad B-D peaks (Figure S7b).

The evidence for isotopic scrambling requires that elimination of molecular hydrogen proceeds by a more complex process than a simple heterolytic DHB promoted process as shown in Scheme 1. A version of the intermediate BH_5, (η^2-H_2)BH_3, may account for the isotopic scrambling observed and also the dependence of the scrambled products on the source of deuterium. BH_5, observed directly in 1994 by infrared spectroscopy,[12g] has been predicted as an intermediate in the hydrolysis of BH_4^-[12a−d] and in the reaction of D_2 and DB.[12e,f] High level quantum chemical studies predict the most stable geometry of BH_5 is a side-on coordinated complex of borane and molecular hydrogen.[13] The (η^2-H_2)B fragment is primarily stabilized by electron donation from the H−H bond to an empty boron 2*p* orbital, forming another version of a 3c−2e bond similar to the bonding in DB.

2.2.4. Theoretical Calculations. Based on theoretical calculations and experimental data, we propose ADB formation mechanisms (Scheme 2) which are much more comprehensive than the original prediction (Scheme 1). The calculated electronic energy barrier (ΔE) and free energy barrier (ΔG) of the different possible pathways at the M062*X*/6-311++G (d,p) level of theory are listed in Table S1. The energy profile is shown in Figure 2.

In the proposed possible formation mechanisms of ADB, the first step of the mechanisms had been predicted theoretically and proved experimentally (Experimental Section and Figure S8, Table S1).[5] From AaDB to the final product ADB, several steps were involved (pathway 1, red label in Scheme 2 and Figure 2). Transition state (TS) structure TS2−1 has a six-membered ring via B_a−N−H···H−B_b−H in which the B_a−O bond distance is 1.99 Å and the H−B_a bond distance is 2.01 Å (Figure 3). A H···H distance of 1.44 Å in the N−H···H−B_b moiety implies that H_2 does not form in this step. The structure

Scheme 2. Proposed Different Formation Mechanisms of ADB

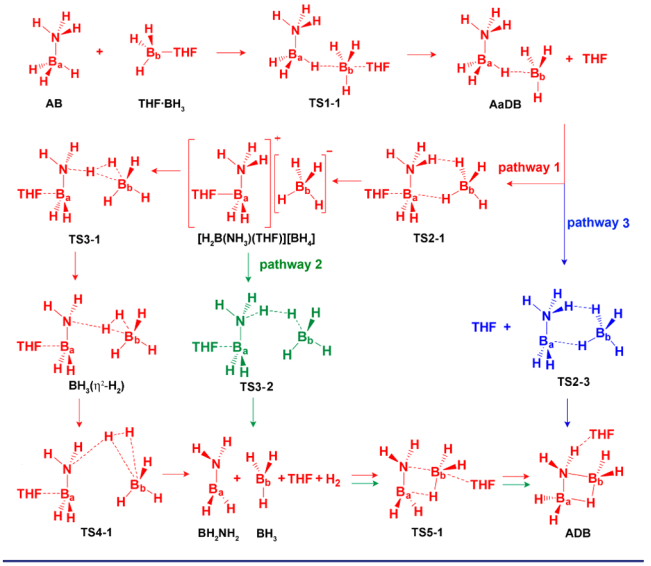

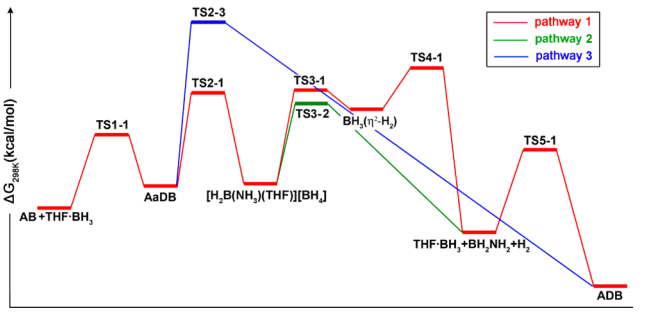

Figure 2. Energy profile of proposed different possible formation mechanisms (in THF solvent).

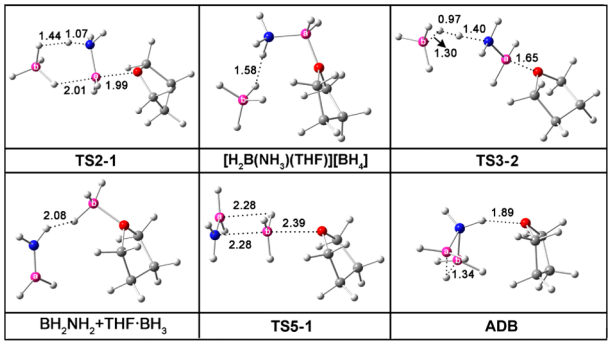

Figure 3. Optimized reaction complexes (RC), TS, and products in the formation pathway 2. Colors: N, blue; B, pink; O, red; H, white; C, gray (bond length is shown in Å).

of TS2−1 was considered the lowest energy barrier to H_2 formation among possible TS structures reported by Dixon et al.[14] Here, the relative energy of TS2−1 to the complex between AB and THF·BH_3 is 29.4 kcal/mol in vacuum. Solvation effects reduce the energy barrier to 21.0 kcal/mol.

In the intermediate ion pair $[H_2B(NH_3)(THF)]^+[BH_4]^-$, an analogue of DADB, the BH_4 moiety is calculated to bear an effectively single negative charge (−0.926) while the H_2B-(NH_3) (THF) moiety carries a corresponding positive charge to form $[H_2B(NH_3)(THF)]^+$. Formation of $[H_2B(NH_3)(THF)]^+[BH_4]^-$ is endothermic by 10.5 kcal/mol in vacuum

DOI: 10.1021/jacs.5b08033
J. Am. Chem. Soc. 2015, 137, 12406−12414

and by 4.0 kcal/mol in THF solvent with respect to the initial complex.

For the TS3−1 (Figure 4), the hydridic H of BH_4^- interacts with the H−N of $[H_2B(NH_3)\ (THF)]^+$ through a B_b−H···H−

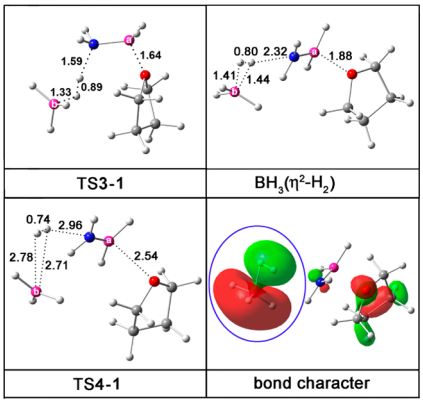

Figure 4. Optimized intermediate BH_3 (η^2-H_2) and TS3−1, TS4−1, and the bond character of η^2-H_2 for the formation pathway 1. Colors: N, blue; B, pink; O, red; H, white; C, gray (bond length is shown in Å).

N DHB interaction, resulting in the formation of $[(THF)BH_2NH_2](\eta^2\text{-}H_2)BH_3$, the intermediate that accounts for scrambling. The two B···H distances (1.41, 1.44 Å) and H···H distance (0.80 Å) demonstrate that the intermediate is a molecular dihydrogen complex. The bonding character between BH_3 and H_2 further confirms the bonding of H_2 (Figure 4). In TS4−1, the H···H distance (0.74 Å) and two B···H distances (2.78 and 2.71 Å) suggest the elimination of H_2 resulting in the formation of AoB and BH_3 moieties and followed by passage through TS5−1. The free energy barrier of TS4−1 is 17.5 kcal/mol in vacuum and 25.4 kcal/mol in THF solvent.

AoB and THF·BH_3 form upon the elimination of H_2. A new complex is formed by DHB interaction between AoB and THF·BH_3, characterized by a H···H distance of 2.08 Å. In TS5−1, the N atom of planar AoB donates its lone pair electrons to the unoccupied 2p orbital of B_b in BH_3. Simultaneously, there is an electrostatic interaction between the B_a site of AoB and H of BH_3. Thus, the four-membered B_a−N−B_b−H ring is formed and finally results in the formation of ADB. The required energy for this step is 3.5 kcal/mol in vacuum and 10.4 kcal/mol in THF solvent related to the initial complex. According to the free energy barriers of the mechanism, the key step is the formation of the transition state TS4−1.

An alternative mechanism is also shown in Scheme 2. The intermediate TS3−2 proceeds directly to AoB and THF·BH_3 (pathway 2, green label in Scheme 2 and Figure 2), after the elimination of H_2, without formation of the intermediate BH_3 (η^2-H_2) and TS4−1. This pathway had been predicted theoretically.[14] In comparison with TS2−1/TS3−2, the energy barrier of TS4−1 is lower than those of TS2−1/TS3−2 in vacuum but higher than those of TS2−1/TS3−2 in solvent. However, the hydrogen scrambling processes resulting in the formation of $BH_3(\eta^2\text{-}H_2)$ support pathway 1.

Both experimental and theoretical studies have ruled out the possibility for AaDB to directly go to ADB via transition state TS2−3 (pathway 3, blue label in Scheme 2 and Figure 2). In pathway 3, the direct formation of an intramolecular DHB in AaDB through B_b-H···H−N would lead to a six-membered ring transition state TS2−3 (Figure S9). The H···H distance is as short as 0.91 Å and the B−H, N−H distances are as long as 1.33 and 1.50 Å, suggesting that the molecular H_2 could be eliminated in this step. The calculated energy barrier of this step, however, is 26.7 kcal/mol in vacuum and 34.2 kcal/mol in THF solvent, which is much higher than those of other proposed transition states. Pathway 3 is therefore not an energetically favored route to ADB. While the relatively strong DHB (0.91 Å H···H distance) and stable chair conformation stabilize the intermediate AaDB, they do not lower the barrier to ADB formation. The formation of H_2, HD, and D_2 in the isotopic labeling experiments demonstrate that hydrogen release is not simply a heterolytic DHB promoted process.

In the proposed formation mechanism of ADB (pathway 1), five intermediates are proposed based on calculations and are consistent with experimental results. Intermediate, AaDB, has been observed experimentally[5] and $[H_2B(NH_3)\ (THF)]^+[BH_4]^-$, an analogue of DADB, was formed in a similar manner to DADB.[5] When NH_3 was bubbled into the reaction mixture to react with AaDB, DADB formed.[5] Similarly, in the reaction of AB and THF·BH_3, THF reacts with AaDB to form $[H_2B(NH_3)\ (THF)]^+[BH_4]^-$.

After transition state TS3−1, the formation of the intermediate boron molecular hydrogen coordination complex $[(THF)BH_2NH_2](\eta^2\text{-}H_2)BH_3$ is supported by the hydrogen scrambling evidence. The formation of hydrogen makes it reasonable to assume that DHB formation precedes hydrogen elimination as suggested by theoretical work (Figures 2, 3, 4, S8, S9). Furthermore, the hydrogen scrambling supports the formation of the boron to molecular hydrogen coordination complex.

Involvement of a BH_5 analogue is shown in Scheme S1. By analogy with the hydrolysis of sodium borohydride in sulfuric acid,[13d] the N−H in $[H_2B(NH_3)\ (THF)]^+[BH_4]^-$, is considered the source of acidic proton. Although much more weakly acidic than H_2SO_4, it is effective in this case since the proton transfer is an intramolecular process. The initial DHB is converted to a (η^2-H_2)B bond and molecular hydrogen is then eliminated to produce AoB and THF·BH_3. In the isotopic labeling experiment NH_3·BH_3 with THF·BD_3, there are two possibilities at this point: (1) HD is eliminated without change in isotope positions and ADB forms, and (2) proton-hydride scrambling is accomplished as the DHB reforms via (η^2-H_2)B. The proton-hydride scrambling leads to the formation of H_2 or D_2 gas and also deuteride signals in the proton position in ^2H NMR due to the reversible process (Scheme S1).

In the final step, H_2 and AoB are formed after TS4−1. Gas release was observed and the hydrogen produced was confirmed by mass spectra (Figure S10). The isotopic experiments further confirmed the formation of H_2, HD, and D_2 (Figure S6a). The formation of the intermediate AoB cannot be observed directly due to its instability. However, a small amount of white precipitate was obtained among the products which was determined to be $(NH_2BH_2)_n$ (Figure S1).[9] According to the mechanism, most of the intermediate AoB was trapped by BH_3 to form ADB while a small amount of AoB oligomerized to $(NH_2BH_2)_n$.

DHB consistently plays an important role in the formation of RC and stabilization of TS and intermediates, as well as in precursors to molecular hydrogen elimination. Where there is no potential for DHB formation, as in the case of *N,N,N*-trimethyl amineborane and THF·BH_3, there is no reaction between the amineborane and THF·BH_3. This pattern had also

DOI: 10.1021/jacs.5b08033
J. Am. Chem. Soc. 2015, 137, 12406−12414

been observed in the reactions of DB with ammonia/*N*-methyl amines to produce a covalent borane adduct, $NH_{(3-n)}Me_n{\cdot}BH_3$, and an ionic product, $[H_2B(NH_{(3-n)}Me_n)_2][BH_4]$ (n = 0, 1, 2, 3) via intermediate AaDB or its *N*-methyl analogues.[7f,15] The ratio of covalent product to ionic product increases with the progressive methylation of amines. For trimethyl amine, only pure trimethylamineborane was produced, a pattern initially explained by trends in steric effects and dielectric constants of amines[16] but more recently attributed to DHB.[5] The results presented here support DHB as the critical factor rather than steric effects or dielectric constant. In these reactions, the opportunity to form a DHB decreases with the progressive substitution of hydrogens on nitrogen, consistent with the observed reaction trends of amineboranes with $THF{\cdot}BH_3$.

2.3. Structural Characteristics and Solution Behavior of ADB. *2.3.1. Structural Characteristics of ADB from X-ray Analysis.* Determination of the structure of ADB has been of interest since its first preparation. A structure, $BH_2NH_2BH_3$, proposed on the basis of the octet rule, was originally reported in 1938 but was not considered definitely proved.[6b] The structure of ADB was first studied by Bauer using electron diffraction, where only the B−N−B skeleton could be determined because of the difficulties in discriminating closely spaced, nonequivalent internuclear distances and the instability of ADB.[17a] As a result, the electron diffraction investigation could not differentiate the configurations $H_3B{-}NH_2{-}BH_2$ from $H_3B{-}NH{-}BH_3$.[17a] In 1952, from electron diffraction in the gas phase, Hedberg and Stosick proposed that the ADB molecule had a symmetrical structure with 4-fold coordination about the nitrogen atom, formally derived from the DB structure by the simple replacement of a bridge hydrogen atom with NH_2.[17b] This symmetrical structure was subsequently supported by microwave spectra and calculations.[17c,d]

In the course of our study, a volatile liquid, ADB·THF,[1a] has been isolated from the reaction of AB and $THF{\cdot}BH_3$, crystallized as needles by careful cooling to 200 K (Experimental Section). The single crystal structure is shown in Figure 5 and the crystallographic data are listed in Table S2.

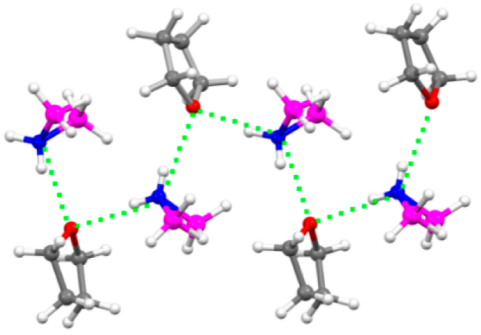

Figure 5. Single crystal structure of ADB·THF. Colors: N, blue; B, pink; O, red; H, white; C, gray (dashed green line shows hydrogen bonds).

The crystal structure of ADB·THF consists of a zigzag chain formed by hydrogen bonding interactions between ADB and THF; that is, the oxygen atom of THF is bonded to hydrogen atoms from NH_2 groups of two adjacent ADB molecules (N−H···O distances range from 2.928 (5) to 3.055 (5) Å). The hydrogen bonding in ADB·THF is similar to that in 2ADB·18-crown-6, in which hydrogen bonding interactions exist between the hydrogen atoms of an NH_2 group and an oxygen atom of 18-crown-6.[1a] DHB may form between the B−H hydride of ADB and a C−H of THF, since this $H^{\delta+}\cdots H^{\delta-}$ distance is 2.18 Å (<2.4 Å, after normalization with N−H = 1.03 and B−H (terminal hydrides) = 1.21 Å, Figure S11d).[18] This alternating hydrogen bonded arrangement of THF and ADB explains why the THF molecule cannot be removed completely to produce pure ADB, as the NMR spectra showed the final product to be a mixture of ADB and THF in 1:1 ratio.[1a] Both the hydrogen bond and DHB help to construct the three-dimensional structure.

Table S3 contains structural parameters for ADB in the crystal obtained from a THF solution, for ADB in crown ether adduct, and for ADB in the gas phase as reported in the literature,[17c] along with the structural parameters of DB.[19a] All bond distances and angles of ADB in the two adducts are comparable and agree within 3 times the standard uncertainty. The bond parameters are also comparable to that in the structure determined in the gas phase.[17c,d] In comparison with DB, the B−B distance in ADB is significantly longer. B−H distances are similar in both DB and ADB. The replacement of one of the bridge hydrogen atoms of DB by an NH_2 group leads to a longer B−B distance in ADB, but has no significant influence on B−H bond lengths. The N−H distances in these structures are comparable.

2.3.2. Solution Behavior of ADB from NMR Analysis. Although the bond distances of ADB and DB in the solid crystalline state are very similar, the two boranes in solution are easily distinguished. The reactivity of ADB is much lower than that of DB. A broad hydride signal was observed at about 1.00 ppm in the $^1H\{^{11}B\}$ NMR spectrum of ADB in THF-d_8 (Figure S12a), indicating that fluxional exchange of terminal and bridge hydrides occurs at room temperature (Scheme S2). No such exchange occurs in less polar toluene-d_8 or diethyl ether-d_{10}. Signals for terminal (1.28 ppm) and bridge hydride (−0.20 ppm) are clearly observed (Figure S12b, c). The chemical shift of the triplet proton signal of NH_2 (Figure S12) is shifted significantly to high field when ether solvents, THF-d_8 or diethyl ether-d_{10}, are replaced by less polar toluene-d_8 in which there is no hydrogen bonding capability.

Variable temperature ^{11}B and $^1H\{^{11}B\}$ NMR analysis of ADB in THF-d_8 (Figure 6) confirmed that hydride exchange was stopped at low temperature. The ^{11}B signal (Figure 6A), a very board triplet at about −27.00 ppm at 30.0 °C, changed to a broad sextet at 41.7 °C, indicating more rapid exchange, and became a sharper triplet at −37.0 °C as exchange stopped. In the $^1H\{^{11}B\}$ NMR spectrum, terminal and bridge hydrogen

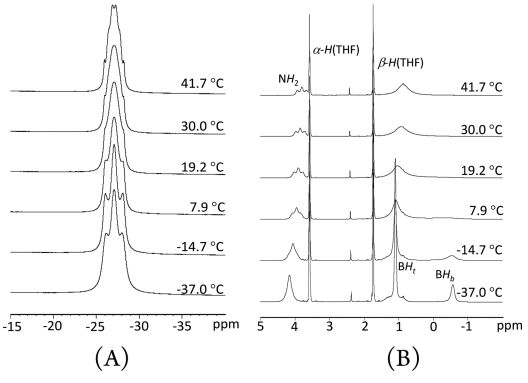

Figure 6. Variable temperature ^{11}B (A) and $^1H\{^{11}B\}$ (B) NMR spectra of ADB in THF-d_8.

DOI: 10.1021/jacs.5b08033
J. Am. Chem. Soc. 2015, 137, 12406−12414

signals were resolved and appeared at 1.15 and −0.55 ppm respectively at low temperature (Figures 6B, S13).

Similar hydride exchange has been reported for DB in diethyl ether.[19b,c] At low temperature, B_2H_6 in diethyl ether exhibited a triplet of triplets which was transformed to a seven-lined spectrum at elevated temperature in ^{11}B NMR spectra. The different solution behaviors of ADB and DB indicates that the replacement of one bridge hydrogen by a NH_2 group strengthens the remaining bridge hydrogen bond.

To estimate the strength of the bridge hydrogen bond in ADB is important for exploring its reactivity. Theoretical results support the conclusion that the B−H−B bridge bond in ADB is stronger than the B−H−B bridge bond in DB. The structures of ADB and DB were optimized by density functional theory (DFT) calculations with no orbital symmetry constraint using the hybrid M062X,[19d] exchange-correlation functional in conjunction with the 6-311++G (d,p) basis set. On the basis of the optimized geometries, the natural bond orders of ADB and DB were calculated by natural resonance theory (NRT) in the NBO program. The detailed NRT bond orders are included in Figure S14 and listed in Table S4. Also, the 3c−2e B−H−B bond character was determined by NBO calculations (Table S4). Consistent with our experimental observations, the computed B−H natural bond order (0.49) in ADB is larger than those in DB (0.33−0.43).

The solution behavior of ADB is similar to that of *N,N*-dimethylaminodiborane.[20] In THF solution, the ^{11}B spectrum of N, N-dimethylaminodiborane displays a sextet at 63 °C, similar to that of ADB, which appears as a broad sextet at 41.7 °C.[20b] The hydrogen exchange of ADB is more rapid than that of N,N-dimethyl aminodiborane,[20b,c] probably due to the hydrogen bond formed between THF and a proton of the NH_2 group of ADB (Scheme S2).

2.4. Reactions of ADB. As a derivative of highly reactive DB, ADB is expected to be chemically active because of its terminal and bridge hydrides and its unstable four-membered ring, but it has been little studied.[1] On the other hand, the maintained four-membered ring structural feature of ADB in THF solution promotes different reactivity of ADB from that of DB because DB cleavages to BH_3 group in basic solvents such as THF and $(CH_3)_2S$. Addition of Lewis bases to ADB produce linear complexes through a nucleophilic scission of a bridging B−H bond in ADB.[1a,c,d] The B, N butane analogue, $NH_3BH_2NH_2BH_3$, was first synthesized by reaction of ADB with NH_3 in which NH_3 opens the four-membered ring of ADB.[1a] The ion pair $[NH_4]^+[BH_3NH_2BH_3]^-$ had been proposed by Schlesinger[21a] and a calculated structure confirmed by Dixon,[21b] but $[NH_4]^+[BH_3NH_2BH_3]^-$ has never been prepared. Although Schlesinger had proposed that the related ion pair $Na[H_2N(BH_3)_2]$ could be prepared by addition of borane to $NaNH_2BH_3$,[21a] $Na[H_2N(BH_3)_2]$ has been prepared only recently by reduction of AB with excess Na in THF or by reaction of 2 equiv of AB with $NaNH_2$ in refluxing THF.[22a,i]

A reaction of NaH with ADB was carried out to determine whether the hydride of NaH reacts with the proton of the NH_2 group or with the boron atom to open the four-membered ring. Experimental result indicates that the ring of ADB opens by hydride addition to boron to produce $Na[H_2N(BH_3)_2]$, eq 1, which is a simple route for preparation of $Na[H_2N(BH_3)_2]$.

$$NaH + NH_2B_2H_5 = Na[H_2N(BH_3)_2] \quad (1)$$

^{11}B and ^1H NMR analysis of the product clearly showed signals associated with amine and borane groups (Experimental Section). An 18-crown-6 ether complex with $Na[H_2N(BH_3)_2]$ formed crystals suitable for X-ray analysis.[1a,23] Single crystal X-ray diffraction analysis showed that the adduct with 18-crown-6, $Na[H_2N(BH_3)_2]$·18-crown-6·2THF, crystallizes in the $P2_1/n$ space group. The structure of this adduct containing the $[NH_2(BH_3)_2]^-$ anion is shown in Figure 7. Crystallographic

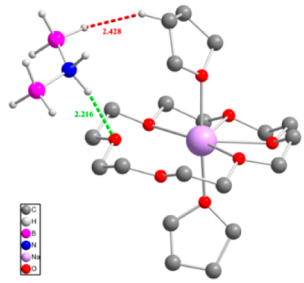

Figure 7. Single crystal structure of $Na[H_2N(BH_3)_2]$ in the $Na[H_2N(BH_3)_2]$·18-crown-6·2THF adduct. Colors: N, blue; B, pink; O, red; H, white; C, gray; Na, purple (bond length is shown in Å).

data are listed in Table S2. The $Na[H_2N(BH_3)_2]$ salt crystallizes with 1 equiv of 18-crown-6 per sodium ion. An NH_2 hydrogen atom is bound to an ether oxygen based on the H···O distance, 2.22 Å. Weak DHBs are present between B−H of $[H_2N(BH_3)_2]^-$ and C−H of THF with an $H^{\delta+}\cdots H^{\delta-}$ distance of about 2.4 Å. Sodium is coordinated to both the 18-crown-6 and the two THF oxygen atoms and the $[H_2N(BH_3)_2]^-$ anion is free, which is different from the transition metal and alkaline earth metal salts of aminodiboranate.[22a−h]

3. CONCLUSIONS

The ready availability of ADB has made it possible to determine important characteristics of this stable nitrogen derivative of DB. AaDB and AoB are key intermediates in the formation of ADB. A concerted reaction in which AaDB directly loses molecular hydrogen to form ADB has been ruled out by a high calculated energy barrier and the observation of protic-hydridic hydrogen exchange during molecular hydrogen elimination. AaDB is transformed to an ion pair, $[H_2B(NH_3)(THF)]^+[BH_4]^-$, which serves as the precursor to an analogue of BH_5 and also illustrates the important role of THF and DHB in several of the transformations we have observed. The ion pair reversibly forms a BH_5-like intermediate, $[(THF)\text{-}BH_2NH_2](\eta^2\text{-}H_2)BH_3$, which is invoked to account for hydrogen/deuterium scrambling observed in the molecular hydrogen products, in ADB and the other reagents. Loss of molecular hydrogen from the ion pair leads to the formation of AoB, most of which is trapped by borane to form ADB, with a small amount oligomerizing to $(NH_2BH_2)_n$. Theoretical calculations were used to test the viability of the proposed intermediates and the related activation processes. The 1:1 ADB·THF complex is consistently obtained. Its structure, as revealed by single crystal X-ray analysis, is a three-dimensional array of zigzag chains of ADB and THF, organized by hydrogen bonds and DHB interactions. THF is also important in the observed room temperature exchange of terminal and bridge hydrogens in ADB. In diethyl ether or toluene exchange does not occur at room temperature. Experimental and theoretical results confirm that the B−H−B bridge in ADB is stronger than those in DB but that this bond is broken when ADB reacts with

DOI: 10.1021/jacs.5b08033
J. Am. Chem. Soc. 2015, 137, 12406−12414

NaH to form sodium aminodiboronate, $Na[NH_2(BH_3)_2]$. The structure of this salt was determined by single crystal X-ray analysis of its 18-crown-6 ether adduct.

4. EXPERIMENTAL SECTION

4.1. General Experimental Details. Unless indicated otherwise, all manipulations were carried out in a high vacuum line or nitrogen-filled glovebox or glovebag. Ammonia borane (AB), sodium hydride (NaH), deuterated ammonia (ND_3), tetrahydrofuran-deuterated borane ($THF{\cdot}BD_3$), methylamine borane, dimethylamine borane, and trimethylamine borane were purchased from Aldrich and used as received without further purification. $THF{\cdot}BH_3$ (Aldrich) was redistilled prior to use and THF (Aldrich) was dried over sodium/benzophenone and freshly distilled prior to use. Crystalline 18-crown-6 ether (Aldrich) was ground to a powder and dried over P_2O_5 under vacuum for 5 days. Dry THF was condensed onto dry 18-crown-6. The mixture was warmed to room temperature, stirred for 10 min, and the THF was evaporated under dynamic vacuum. THF replacement was repeated twice, after which there was no observable water signal in the ^1H NMR spectrum of the crown ether.

All reactions were monitored by ^{11}B NMR spectroscopy which easily distinguishes AB, ADB and $THF{\cdot}BH_3$. Product ratios in reactions of AB and *N*-methyl amineboranes with $THF{\cdot}BH_3$ were calculated based upon the integrated values of the corresponding boron signals in ^{11}B or $^{11}B\{^1H\}$ NMR spectra (Figures S2−S5). The ^1H and $^1H\{^{11}B\}$ NMR spectra were recorded at 500 MHz and externally referenced to residual solvent. The ^{11}B and $^{11}B\{^1H\}$ NMR spectra were obtained at 160 MHz and externally referenced to $BF_3{\cdot}OEt_2$ in C_6D_6 (δ = 0.00 ppm). ^2H NMR spectra were recorded at 76.77 MHz on a Bruker DRX-500 spectrometer. Infrared (IR) spectra with 4 cm^{-1} resolution were recorded using a GladiATR (Pike Technologies) ATR accessory protected by a glovebox. Mass spectra of gases released from the reactions were determined using a Balzers Quadstar 422 quadrupole mass spectrometer. Powder XRD data for small amount of white powder from the reaction of AB and $THF{\cdot}BH_3$ was collected on a Bruker advance-D8 diffractometer (40 kV, 100 mA, Cu Kα_1 radiation) over the range of 2θ = 5−80° at room temperature.

4.2. X-ray Crystallography. Crystal structure data were collected on a Nonius Kappa CCD diffractometer, equipped with graphite-monochromated Mo Kα radiation (λ = 0.71073 Å) and an Oxford Cryosystems Cryostream Cooler. Crystallographic details for ADB·THF and $Na[H_2N(BH_3)_2]{\cdot}$18-crown-6·2THF are listed in Table S2.

For ADB·THF, X-ray quality crystals were grown in a capillary mounted in the cold nitrogen gas stream on the diffractometer, since the sample is a liquid at room temperature. The sample was condensed into a Pyrex sample tube, which consisted of a capillary about 1 mm in diameter attached to a bulb about 1 cm in diameter. A very small part of the sample at the bottom end of the capillary was sealed in the capillary, and then placed in the cold gas stream on the diffractometer. With much patience and persistence a single crystal of appropriate quality was eventually obtained by slowly lowering and raising the temperature of the gas stream several times.

All work was performed at 200 K using an Oxford Cryosystems Cryostream Cooler. Phi and omega scans with a frame width of 1.0° were used for data collection. Data integration was done with Denzo,[24] and scaling and merging of the data was done with Scalepack.[24] Because of the weakness of the diffraction pattern, data was collected only out to 2θ of 45°.

The structure was solved by direct methods in SHELXT-2014/5.[25a] The asymmetric unit consists of two half aminodiborane molecules, $NH_2B_2H_5$, each one sitting on a crystallographic mirror plane, and two half THF molecules, with each one also containing a mirror plane. Full-matrix least-squares refinements based on F^2 were performed in SHELXL-2014/7,[25b] as incorporated in the WinGX package.[25c]

One of the THF molecules is disordered and was modeled with two positions for one carbon atom, C (4A) and C (4B). Anisotropic displacement parameter restraints (RIGU) were used for atoms C (3), C (4A) and C (4B) in the least-squares refinement. The hydrogen atoms on both ADB molecules were refined isotropically. The remaining hydrogen atoms were included in the model at calculated positions using a riding model with U (H) = 1.2 * Ueq (bonded atom).

The crystals of $Na[H_2N(BH_3)_2]{\cdot}$18-crown-6·2THF are colorless plates. All work was done at 150 K using an Oxford Cryosystems Cryostream Cooler. The data collection strategy was set up to measure a quadrant of reciprocal space with a redundancy factor of 3.5, which means that 90% of these reflections were measured at least 3.5 times. Phi and omega scans with a frame width of 1.0° were used. Data integration was done with Denzo,[24] and scaling and merging of the data was done with Scalepack.[24]

The structure was solved by direct methods in SHELXS-2013/1.[25b] Full-matrix least-squares refinements based on F^2 were performed in SHELXL version 2014/3,[25b] as incorporated in the WinGX package.[25c]

One of the THF molecules is disordered and was modeled with two orientations for the whole molecule. Distance restraints (SADI) and restraints on the anisotropic displacement parameters (RIGU) were used in the least-squares refinement. The occupancy factors for these two molecules refined to 0.61 (1) and 0.39 (1).

The hydrogen atoms on the ADB anion were refined isotropically. One of the hydrogen atoms bonded to the nitrogen is involved in an intermolecular hydrogen bond with an oxygen atom, O (3), of the crown ether. The remaining hydrogen atoms were included in the model at calculated positions using a riding model with U (H) = 1.2 * Ueq (bonded atom).

4.3. Computational Details. All DFT calculations were performed using the Gaussian 09W program.[26] The geometries were optimized at M062*X*/6-311++G(d,p) level of theory. M062X functional was proved to be very accurate for reproducing the thermodynamic data, barrier heights, and isomerization energies.[19d,27] The vibrational frequency was calculated at the same level to determine whether it is an equilibrium structure or a transition state (TS). The corresponding normal mode for the imaginary vibrational frequency then suggested the related reactant and product for that TS. Natural population analysis (NPA) was used to evaluate the atomic charge of the models. Electronic energy (ΔE, kcal/mol at 0 K) and Gibbs free energy (ΔG, kcal/mol at 298 K) barriers can be used to discuss the reaction between AB and $THF{\cdot}BH_3$ to produce ADB. The solvation effect in THF was considered by the SMD solvation model,[28] which is a recommended program to compute the ΔG of solvation. Single point energy calculations with SMD approach were carried out using the fully optimized geometries in vacuum. The Cartesian coordinates and vibrational frequencies of the studied models are listed in the Supporting Information.

4.4. Scrambling between Proton and Hydride. The proton/hydride scrambling reaction was studied by isotopic labeling experiments. The starting materials comprised two groups: $ND_3{\cdot}BH_3$ + $THF{\cdot}BH_3$ and $NH_3{\cdot}BH_3$ + $THF{\cdot}BD_3$. $ND_3{\cdot}BH_3$ was prepared using ND_3 instead of NH_3.[12] The gaseous hydrogen products were identified by mass spectrometry after separation from the solution mixture using a Toepler pump. The solution mixtures were monitored by ^2H NMR spectroscopy (Figures S6, S7).

4.5. Reactions of *N*-Methyl Amineboranes with $THF{\cdot}BH_3$. The reactions of AB and *N*-methyl amineboranes with $THF{\cdot}BH_3$ were carried out according to the literature.[1a] All reactions were monitored using ^{11}B NMR spectroscopy. The conversion of the reaction was calculated based on ratios of product and starting materials from the integration of the corresponding boron signals in ^{11}B NMR spectra (Figures S2−S5).

4.6. Synthesis of Sodium Aminodiborate $Na[H_2N(BH_3)_2]$. In a drybox, a 50 mL flask was charged with sodium hydride (NaH, 0.41 g, 17 mmol). The flask was connected to a vacuum line and ca. 17 mL of 1 M THF solution of ADB (ADB·THF, 17 mmol) was condensed into it. The reaction mixture was stirred for 4 h at 0 °C, a small amount of white solid was separated by filtration, and then the THF was removed from the filtrate under vacuum. White powder was produced in 76% yield (0.86 g). ^1H NMR (d_6-DMSO, 500 MHz) δ 3.30 (*br s*, 3H of NH_2) ppm, δ 1.50, 1.31, 1.14, 0.96 (q, BH_3, $J_{B-H} \approx 90$ Hz) ppm. ^{11}B (d_6-DMSO, 160 MHz) δ −17.87, −18.44, −19.00, −19.55 (*q*, BH_3,

DOI: 10.1021/jacs.5b08033
J. Am. Chem. Soc. 2015, 137, 12406−12414

$J_{B-H} \approx 90$ Hz) ppm. ATR: ν (N−H): 3307 (s), 3263 (m) cm^{-1}; ν (B−H): 2218 (s, broad), 1556 (s), 1225 (s), 1170 (s), 1054 (s), 1019 (s), 905 (s), 869 (w), 748 (w), 666 (w) cm^{-1}.

4.7. Synthesis of an Adduct of 18-Crown-6 with $Na[H_2N(BH_3)_2]$. A 10 mL THF solution of $Na[H_2N(BH_3)_2]$ (0.335 g, 0.5 mmol) was prepared, and 0.13 g (0.5 mmol) of dry 18-crown-6 was added to the solution in a drybox. The mixture was stirred for 5 min and filtered. The clear solution was kept in the refrigerator at −30 °C, and X-ray quality crystals were obtained from the above solution after 25 days.

■ ASSOCIATED CONTENT

Supporting Information

The Supporting Information is available free of charge on the ACS Publications website at DOI: 10.1021/jacs.5b08033.

Details for experimental, computational, and crystallographic work (PDF)
Crystallographic data (CIF)

■ AUTHOR INFORMATION

Corresponding Authors

*jie.zhang@htu.edu.cn
*zhao.199@osu.edu
*xnchen@htu.edu.cn

Author Contributions

⊥H. Li and N. Ma contributed equally.

Notes

The authors declare no competing financial interest.

■ ACKNOWLEDGMENTS

The authors from HNU are grateful for the financial support from the National Natural Science Foundation of China (Grant Nos. 21371051, 21401047, 21571052, 21501048). The work at OSU was supported by the U.S. Department of Energy, Office of Energy Efficiency and Renewable Energy, under Contract No. DE-FC3605GO15062. The authors are grateful to Profs. Thomas Evans and Ewan Hamilton for very valuable comments.

■ DEDICATION

This paper is dedicated to the memory of Professor Sheldon G. Shore.

■ REFERENCES

(1) (a) Chen, X.; Zhao, J.-C.; Shore, S. G. *J. Am. Chem. Soc.* **2010**, *132*, 10658−10659. (b) Wrackmeyer, B.; Molla, E.; Thoma, P.; Klimkina, E. V.; Tok, O. L.; Bauer, T.; Kempe, R. *Z. Anorg. Allg. Chem.* **2011**, *637*, 401−405. (c) Malcolm, A. C.; Sabourin, K. J.; McDonald, R.; Ferguson, M. J.; Rivard, E. *Inorg. Chem.* **2012**, *51*, 12905−12916. (d) Helten, H.; Robertson, A. P. M.; Staubitz, A.; Vance, J. R.; Haddow, M. F.; Manners, I. *Chem. - Eur. J.* **2012**, *18*, 4665−4680. (e) Robertson, A. P. M.; Leitao, E. M.; Jurca, T.; Haddow, M. F.; Helten, H.; Lloyd-Jones, G. C.; Manners, I. *J. Am. Chem. Soc.* **2013**, *135*, 12670−12683.

(2) (a) Burg, A. B.; Randolph, C. L. *J. Am. Chem. Soc.* **1949**, *71*, 3451−3455. (b) Burg, A. B. *J. Am. Chem. Soc.* **1952**, *74*, 1340−1341. (c) Spielman, J. R. *J. Chem. Educ.* **1970**, *47*, 225−226.

(3) (a) Schwartz, L. D.; Keller, P. C. *J. Am. Chem. Soc.* **1972**, *94*, 3015−3018. (b) Schaeffer, G. E.; Basile, L. J. *J. Am. Chem. Soc.* **1955**, *77*, 331−332. (c) Denton, D. L.; Johnson, A. D., II; Hickam, C. W., Jr.; Bunting, R. K.; Shore, S. G. *J. Inorg. Nucl. Chem.* **1975**, *37*, 1037−1038. (d) Böddeker, K. W.; Shore, S. G.; Bunting, R. K. *J. Am. Chem. Soc.* **1966**, *88*, 4396−4401. (e) Keller, P. C. *J. Am. Chem. Soc.* **1969**, *91*, 1231. (f) Keller, P. C. *Synth. React. Inorg. Met.-Org. Chem.* **1973**, *3*, 307−312.

(4) (a) Li, J.; Kathmann, S. M.; Schenter, G. K.; Gutowski, M. *J. Phys. Chem. C* **2007**, *111*, 3294−3299. (b) Wiberg, E.; Bolz, A.; Buchheit, P. *Z. Anorg. Chem.* **1948**, *256*, 285−306. (c) Schaeffer, G. W.; Adams, M. D.; Koenig, F. J.; Koenig, S. J. *J. Am. Chem. Soc.* **1956**, *78*, 725−728. (d) McGee, H. A., Jr.; Kwon, C. T. *Inorg. Chem.* **1970**, *9*, 2458−2461.

(5) Chen, X.; Bao, X.; Zhao, J.-C.; Shore, S. G. *J. Am. Chem. Soc.* **2011**, *133*, 14172−14175.

(6) (a) Schlesinger, H. I.; Ritter, D. M.; Burg, A. B. *J. Am. Chem. Soc.* **1938**, *60*, 1296−1300. (b) Schlesinger, H. I.; Ritter, D. M.; Burg, A. B. *J. Am. Chem. Soc.* **1938**, *60*, 2297−2300.

(7) (a) Li, J.; Kathmann, S. M.; Hu, H.-S.; Schenter, G. K.; Autrey, T.; Gutowski, M. *Inorg. Chem.* **2010**, *49*, 7710−7720. (b) Custelcean, R.; Jackson, J. E. *Chem. Rev.* **2001**, *101*, 1963−1980. (c) Sumerin, V.; Schulz, F.; Atsumi, M.; Wang, C.; Nieger, M.; Leskela, M.; Repo, T.; Pyykko, P.; Rieger, B. *J. Am. Chem. Soc.* **2008**, *130*, 14117−14119. (d) Sumerin, V.; Schulz, F.; Nieger, M.; Atsumi, M.; Wang, C.; Leskela, M.; Pyykko, P.; Repo, T.; Rieger, B. *J. Organomet. Chem.* **2009**, *694*, 2654−2660. (e) Abboud, J.-L. M.; Nemeth, B.; Guillemin, J.-C.; Burk, P.; Adamson, A.; Nerut, E. R. *Chem. - Eur. J.* **2012**, *18*, 3981−3991. (f) Chen, X.; Bao, X.; Billet, B.; Shore, S. G.; Zhao, J.-C. *Chem. - Eur. J.* **2012**, *18*, 11994−11999. (g) Chen, X.; Zhao, J.-C.; Shore, S. G. *Acc. Chem. Res.* **2013**, *46*, 2666−2675. (h) Chernichenko, K.; Kótai, B.; Pápai, I.; Zhivonitko, V.; Nieger, M.; Leskelä, M.; Repo, T. *Angew. Chem., Int. Ed.* **2015**, *54*, 1749−1753.

(8) (a) Tague, T. J., Jr.; Andrews, L. *J. Am. Chem. Soc.* **1994**, *116*, 4970−4976. (b) Sivaev, I. B.; Petrovskii, P. V.; Filin, A. M.; Shubina, E. S.; Bregadze, V. I. *Russ. Chem. Bull.* **2001**, *50*, 1115−1116. (c) Epstein, L. M.; Shubina, E. S. *Coord. Chem. Rev.* **2002**, *231*, 165−181. (d) Belkova, N. V.; Shubina, E. S.; Epstein, L. M. *Acc. Chem. Res.* **2005**, *38*, 624−631. (e) Filippov, O. A.; Filin, A. M.; Tsupreva, V. N.; Belkova, N. V.; Lledos, A.; Ujaque, G.; Epstein, L. M.; Shubina, E. S. *Inorg. Chem.* **2006**, *45*, 3086−3096. (f) Filippov, O. A.; Belkova, N. V.; Epstein, L. M.; Shubina, E. S. *J. Organomet. Chem.* **2013**, *747*, 30−42. (g) Houghton, A. Y.; Karttunen, V. A.; Fan, C.; Piers, E. W.; Tuononen, H. M. *J. Am. Chem. Soc.* **2013**, *135*, 941−947. (h) Belkova, N. V.; Bakhmutova-Albert, E. V.; Gutsul, E. I.; Bakhmutov, V. I.; Golub, I. E.; Filippov, O. A.; Epstein, L. M.; Peruzzini, M.; Rossin, A.; Zanobini, F.; Shubina, E. S. *Inorg. Chem.* **2014**, *53*, 1080−1090.

(9) Staubitz, A.; Sloan, M. E.; Robertson, A. P. M.; Friedrich, A.; Schneider, S.; Gates, P. J.; Günne, J. S.; Manners, I. *J. Am. Chem. Soc.* **2010**, *132*, 13332−13345.

(10) (a) Pons, V.; Baker, R. T.; Szymczak, N. K.; Heldebrant, D. J.; Linehan, J. C.; Matus, M. H.; Grant, D. J.; Dixon, D. A. *Chem. Commun.* **2008**, 6597−6599. (b) Shrestha, R. P.; Diyabalanage, H. V. K.; Semelsberger, T. A.; Ott, K. C.; Burrell, A. K. *Int. J. Hydrogen Energy* **2009**, *34*, 2616−2621. (c) Chapman, A. M.; Haddow, M. F.; Wass, D. F. *J. Am. Chem. Soc.* **2011**, *133*, 8826−8829. (d) Robertson, A. P. M.; Leitao, E. M.; Manners, I. *J. Am. Chem. Soc.* **2011**, *133*, 19322−19325.

(11) (a) Chen, X.; Bao, X.; Billet, B.; Shore, S. G.; Zhao, J.-C. *Chem. - Eur. J.* **2012**, *18*, 11994−11999. (b) $ND_3{\cdot}BH_3$ was prepared using ND_3 instead of NH_3, for comparison. ^{1}H NMR spectrum of $NH_3{\cdot}BH_3$ in CD_3CN was carried out on a Bruker DRX-500 spectrometer: δ 3.69, 3.60, 3.50 (t, 3H of NH_2) ppm, δ 1.66, 1.47, 1.28, 1.09 (q, BH_3, $J_{B-H} \approx$ 90 Hz) ppm..

(12) (a) Mesmer, R. E.; Jolly, W. L. *Inorg. Chem.* **1962**, *1*, 608−612. (b) Davis, R. E.; Bromels, E.; Kibby, C. L. *J. Am. Chem. Soc.* **1962**, *84*, 885−892. (c) Kreevoy, M. M.; Hutchins, J. E. C. *J. Am. Chem. Soc.* **1972**, *94*, 6371−6376. (d) Olah, G. A.; Westerman, P. W.; Mo, Y. K.; Klopman, G. *J. Am. Chem. Soc.* **1972**, *94*, 7859−7862. (e) Webb, A. N.; Neu, J. T.; Pitzer, K. S. *J. Chem. Phys.* **1949**, *17*, 1007−1011. (f) Muetterties, E. L. *J. Am. Chem. Soc.* **1969**, *91*, 1636−1643. (g) Tague, T. J.; Andrews, L. *J. Am. Chem. Soc.* **1994**, *116*, 4970−4976.

(13) (a) Stanton, J. F.; Lipscomb, W. N.; Bartlett, R. J. *J. Am. Chem. Soc.* **1989**, *111*, 5173−5180. (b) Schreiner, P. R.; Schaefer, H. F.; Schleyer, P. v. R. *J. Chem. Phys.* **1994**, *101*, 7625−7632. (c) Watts, J. D.; Bartlett, R. J. *J. Am. Chem. Soc.* **1995**, *117*, 825−826. (d) Kim, Y.;

DOI: 10.1021/jacs.5b08033
J. Am. Chem. Soc. 2015, 137, 12406−12414

Kim, J.; Kim, K. H. *J. Phys. Chem. A* **2003**, *107*, 301−305. (e) Schuurman, M. S.; Allen, W. D.; Schleyer, P. v. R.; Schaefer, H. F. *J. Chem. Phys.* **2005**, *122*, 104302−104311.
(14) Nguyen, M. T.; Nguyen, V. S.; Matus, M. H.; Gopakumar, G.; Dixon, D. A. *J. Phys. Chem. A* **2007**, *111*, 679−690.
(15) Shore, S. G.; Hall, C. L. *J. Am. Chem. Soc.* **1967**, *89*, 3947−3948.
(16) (a) Shore, S. G.; Parry, R. W. *J. Am. Chem. Soc.* **1958**, *80*, 8−12. (b) Shore, S. G.; Parry, R. W. *J. Am. Chem. Soc.* **1958**, *80*, 12−15. (c) Parry, R. W.; Shore, S. G. *J. Am. Chem. Soc.* **1958**, *80*, 15−20. (d) Shore, S. G.; Girardot, P. R.; Parry, R. W. *J. Am. Chem. Soc.* **1958**, *80*, 20−24. (e) Parry, R. W.; Kodama, G.; Schultz, D. R. *J. Am. Chem. Soc.* **1958**, *80*, 24−27. (f) Shore, S. G.; Hickam, C. W., Jr.; Cowles, D. *J. Am. Chem. Soc.* **1965**, *87*, 2755−2756. (g) Young, D. E.; Shore, S. G. *J. Am. Chem. Soc.* **1969**, *91*, 3497−3504.
(17) (a) Bauer, S. H. *J. Am. Chem. Soc.* **1938**, *60*, 524−530. (b) Hedberg, K.; Stosick, A. J. *J. Am. Chem. Soc.* **1952**, *74*, 954−958. (c) Lau, K.-K.; Burg, A. B.; Beaudet, R. A. *Inorg. Chem.* **1974**, *13*, 2787−2791. (d) Armstrong, D. R. *Inorg. Chim. Acta* **1976**, *18*, 145−146.
(18) (a) Richardson, T. B.; de Gala, S.; Crabtree, R. H.; Siegbahn, P. E. M. *J. Am. Chem. Soc.* **1995**, *117*, 12875−12876. (b) Klooster, W. T.; Koetzle, T. F.; Siegbahn, P. E. M.; Richardson, T. B.; Crabtree, R. H. *J. Am. Chem. Soc.* **1999**, *121*, 6337−6343. (c) Jeffrey, G. A.; Saenger, W. *Hydrogen bonding in biological structure*; Springer: Berlin, 1994.
(19) (a) Smith, H. W.; Lipscomb, W. N. *J. Chem. Phys.* **1965**, *43*, 1060−1064. (b) Gaines, D. F. *Inorg. Chem.* **1963**, *2*, 523−526. (c) Fratiello, A.; Onak, T. P.; Schuster, R. E. *J. Am. Chem. Soc.* **1968**, *90*, 1194−1198. (d) Zhao, Y.; Truhlar, D. G. *J. Phys. Chem. A* **2006**, *110*, 5121−5129.
(20) (a) Phillips, W. D.; Miller, H. C.; Muetterties, E. L. *J. Am. Chem. Soc.* **1959**, *81*, 4496−4500. (b) Gaines, D. F.; Schaeffer, R. *J. Am. Chem. Soc.* **1964**, *86*, 1505−1507. (c) Schirmer, R. E.; Noggle, J. H.; Gaines, D. F. *J. Am. Chem. Soc.* **1969**, *91*, 6240−6246.
(21) (a) Schlesinger, H. I.; Burg, A. B. *J. Am. Chem. Soc.* **1938**, *60*, 290−299. (b) Nguyen, V. S.; Matus, M. H.; Grant, D. J.; Nguyen, M. T.; Dixon, D. A. *J. Phys. Chem. A* **2007**, *111*, 8844−8856.
(22) (a) Daly, S. R.; Bellott, B. J.; Kim, D. Y.; Girolami, G. S. *J. Am. Chem. Soc.* **2010**, *132*, 7254−7255. (b) Daly, S. R.; Girolami, G. S. *Inorg. Chem.* **2010**, *49*, 4578−4585. (c) Kim, D. Y.; Girolami, G. S. *Inorg. Chem.* **2010**, *49*, 4942−4948. (d) Daly, S. R.; Girolami, G. S. *Inorg. Chem.* **2010**, *49*, 5157−5166. (e) Daly, S. R.; Girolami, G. S. *Chem. Commun.* **2010**, *46*, 407−408. (f) Daly, S. R.; Piccoli, P. M. B.; Schultz, A. J.; Todorova, T. K.; Gagliardi, L.; Girolami, G. S. *Angew. Chem., Int. Ed.* **2010**, *49*, 3379−3381. (g) Daly, S. R.; Bellott, B. J.; Nesbit, M. A.; Girolami, G. S. *Inorg. Chem.* **2012**, *51*, 6449−6459. (h) Daly, S. R.; Kim, D. Y.; Girolami, G. S. *Inorg. Chem.* **2012**, *51*, 7050−7065. (i) Dunbar, A. C.; Girolami, G. S. *Inorg. Chem.* **2014**, *53*, 888−896. (j) Chen, W. D.; Huang, Z. G.; Wu, G. T.; Chen, P. *Sci. China: Chem.* **2015**, *58*, 169−173.
(23) (a) Yoon, C. W.; Carroll, P. J.; Sneddon, L. G. *J. Am. Chem. Soc.* **2009**, *131*, 855−864. (b) Chen, X.; Gallucci, J.; Campana, C.; Huang, Z.; Lingam, H. K.; Shore, S. G.; Zhao, J.-C. *Chem. Commun.* **2012**, *48*, 7943−7945.
(24) Otwinowski, Z.; Minor, W. Methods in Enzymology. *Macromolecular Crystallography, part A*; Carter, C. W., Jr., Sweet, R. M., Eds.; Academic Press: New York, 1997; Vol. *276*, pp 307−326.
(25) (a) SHELXT: Sheldrick, G. M. *Acta Crystallogr., Sect. A: Found. Adv.* **2015**, *A71*, 3−8. (b) SHELXL-2014: Sheldrick, G. M. *Acta Crystallogr., Sect. A: Found. Crystallogr.* **2008**, *A64*, 112−122. (c) Farrugia, L. J. *J. Appl. Crystallogr.* **2012**, *45*, 849−854.
(26) Frisch, M. J.; Trucks, G. W.; Schlegel, H. B.; Scuseria, G. E.; Robb, M. A.; Cheeseman, J. R.; Scalmani, G.;Barone, V.; Mennucci, B.; Petersson, G. A.; Nakatsuji, H.; Caricato, M.; Li, X.; Hratchian, H. P.; Izmaylov, A. F.; Bloino, J.; Zheng, G.; Sonnenberg, J. L.; Hada, M.; Ehara, M.; Toyota, K.; Fukuda, R.; Hasegawa, J.; Ishida, M.; Nakajima, T.; Honda, Y.; Kitao, O.; Nakai, H.; Vreven, T.; Montgomery, J. A., Jr.; Peralta, J. E.; Ogliaro, F.; Bearpark, M.; Heyd, J. J.; Brothers, E.; Kudin, K. N.; Staroverov, V. N.; Kobayashi, R.; Normand, J.; Raghavachari, K.; Rendell, A.; Burant, J. C.; Iyengar, S. S.; Tomasi, J.; Cossi, M.; Rega, N.; Millam, J. M.; Klene, M.; Knox, J. E.; Cross, J. B.; Bakken, V.; Adamo, C.; Jaramillo, J.; Gomperts, R.; Stratmann, R. E.; Yazyev, O.; Austin, A. J.; Cammi, R.; Pomelli, C.; Ochterski, J. W.; Martin, R. L.; Morokuma, K.; Zakrzewski, V. G.; Voth, G. A.; Salvador, P.; Dannenberg, J. J.; Dapprich, S.; Daniels, A. D.; Farkas, O.; Foresman, J. B.; Ortiz, J. V.; Cioslowski, J.; Fox, D. J. *Gaussian 09*, Revision D.01; Gaussian, Inc.: Wallingford, CT, 2009.
(27) Zhao, Y.; Truhlar, D. G. *Theor. Chem. Acc.* **2008**, *120*, 215−241.
(28) Marenich, A. V.; Cramer, C. J.; Truhlar, D. G. *J. Phys. Chem. B* **2009**, *113*, 6378−6396.

DOI: 10.1021/jacs.5b08033
J. Am. Chem. Soc. 2015, 137, 12406−12414